Deep-Sea Research Part I 125 (2017) 65–80

Contents lists available at ScienceDirect

Deep-Sea Research Part I

journal homepage: www.elsevier.com/locate/dsri

Environmental and bathymetric influences on abyssal bait-attending communities of the Clarion Clipperton Zone

Astrid B. Leitner*, Anna B. Neuheimer, Erica Donlon, Craig R. Smith, Jeffrey C. Drazen

University of Hawaii Manoa, Department of Oceanography, 1000 Pope Rd., Honolulu, HI 96822, USA

ARTICLE INFO

Keywords:
Clarion Clipperton Zone CCZ
Manganese nodule
Scavenger
Baited camera
Abyssal hill
Deep-sea mining impacts

ABSTRACT

The Clarion-Clipperton Zone (CCZ) is one of the richest manganese nodule provinces in the world and has recently become a focus area for manganese nodule mining interests. However, this vast area remains poorly studied and highly undersampled. In this study, the abyssal bait-attending fauna is documented for the first time using a series of baited camera deployments in various locations across the CCZ. A bait-attending community intermediate between those typical of the California margin and Hawaii was found in the larger CCZ area, generally dominated by rattail fishes, dendrobranchiate shrimp, and zoarcid and ophidiid fishes. Additionally, the western and eastern ends of the CCZ had different communities, with the western region characterized by decreased dominance of rattails and small shrimps and increased dominance of ophidiids (especially *Bassozetus* sp. and *Barathrites iris*) and large shrimps. This trend may be related to increasing distance from the continental margin. We also test the hypothesis that bait-attending communities change across the CCZ in response to key environmental predictors, especially topography and nodule cover. Our analyses showed that higher nodule cover and elevated topography, as quantified using the benthic positioning index (BPI), increase bait-attending community diversity. Elevated topography generally had higher relative abundances, but taxa also showed differing responses to the BPI metric and bottom temperature, causing significant community compositional change over varying topography and temperatures. Larger individuals of the dominant scavenger in the CCZ, *Coryphaenoides* spp., were correlated with areas of higher nodule cover and with abyssal hills, suggesting these areas may be preferred habitat. Our results suggest that nodule cover is important to all levels of the benthic ecosystem and that nodule mining could have negative impacts on even the top-level predators and scavengers in the CCZ. Additionally, there is continuous change in diversity, dominance, and relative abundance across the CCZ and across gradients in bathymetric and oceanographic variables. This work increased the understanding of the biogeography of the demersal scavengers and top predators as well as the key environmental drivers of their distributions across the CCZ in order to better predict and manage the impacts of nodule mining.

1. Introduction

The Clarion-Clipperton Zone (CCZ) is one of the largest and most resource-rich manganese nodule provinces in the world (Fig. 1) and has recently become the focal point for nodule mining interests (Wedding et al., 2015; Mewes et al., 2014). Though there were some mining-motivated, exploratory scientific surveys in the 1980s, until very recently, the biology of this area was largely unexplored (Mewes et al., 2014). In 2015, for example, the Ocean Biogeographic Information System (OBIS) had only 34 records from the entire eastern CCZ, an area of over one million square kilometers. In the last three years, there has been a surge in research in the CCZ due to new nodule-mining exploration licenses granted by the International Seabed Authority (ISA) (Wedding et al., 2015). Much of this research is designed to establish ecological baselines for exploration claims according to ISA requirements aiming to conserve the seabed, dubbed the "Common Heritage of Mankind" (Wedding et al., 2013, UNCLOS XI 1982). Robust ecological baseline surveys that sample all aspects of an ecosystem are crucial to effective and systematic ecosystem-based management (Wedding et al., 2013). Implementing an effective management strategy will also depend on the understanding of key environmental drivers of these communities, especially the importance of the nodules themselves to the community, which is still lacking for this region (Danovaro et al., 2017).

Baited cameras are essential tools for studying abyssal fish and bait-attending communities in general (eg. Bailey et al., 2007a; Yeh and

* Corresponding author.
E-mail addresses: aleitner@hawaii.edu (A.B. Leitner), annabn@hawaii.edu (A.B. Neuheimer), edonlon@hawaii.edu (E. Donlon), craigsmi@hawaii.edu (C.R. Smith), jdrazen@hawaii.edu (J.C. Drazen).

http://dx.doi.org/10.1016/j.dsr.2017.04.017
Received 4 November 2016; Received in revised form 26 April 2017; Accepted 26 April 2017
Available online 03 May 2017

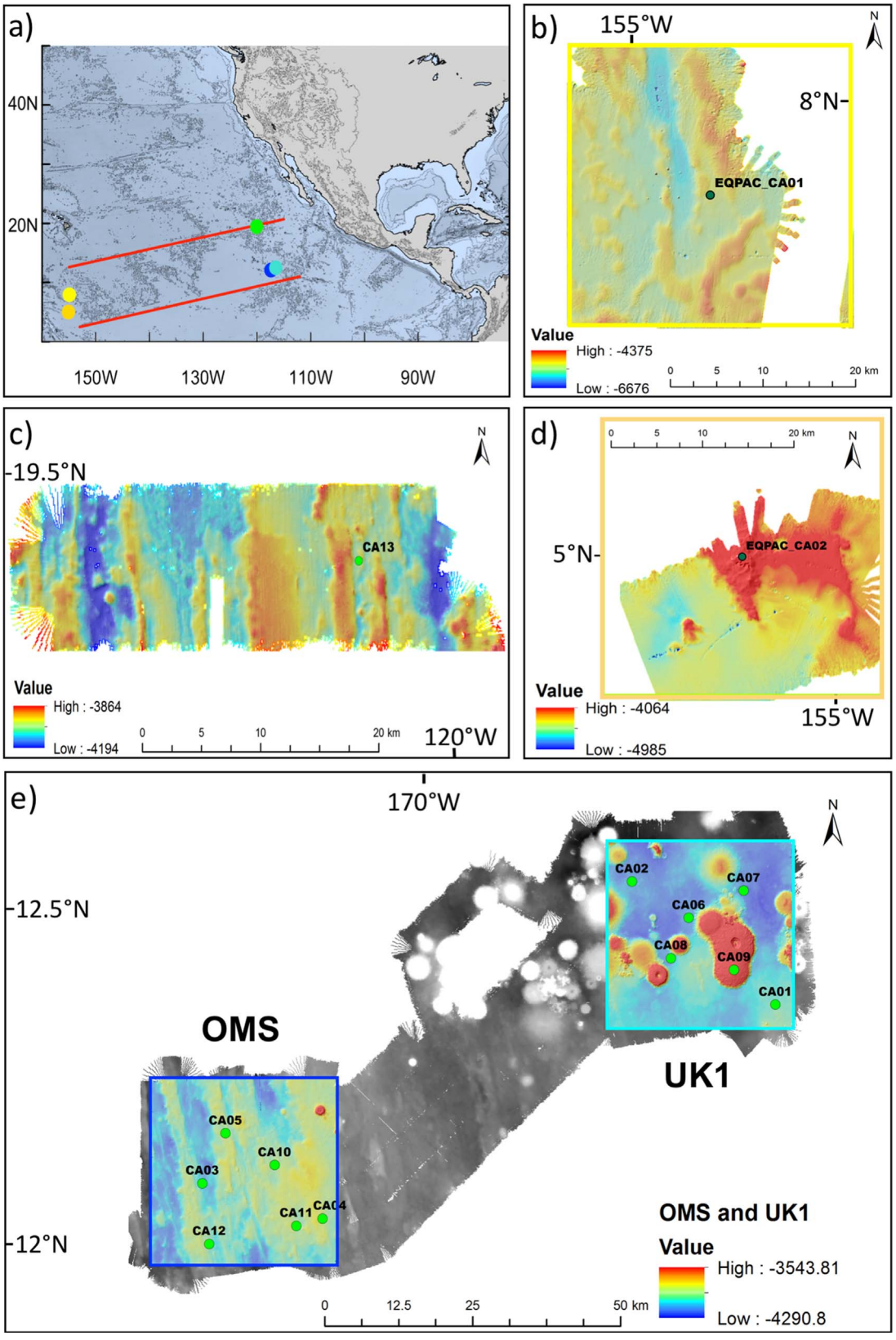

Fig. 1. Maps of the five study areas: (a) a world map with the boundaries of the CCZ in red and deployment locations color-coded by region (green = northern, blues = eastern, yellows = western), (b) the area around stratum EQPAC1 (c) bathymetry of the study area in stratum APEI 6 (d) the area around stratum EQPAC2 (e) Eastern CCZ: OMS stratum (lower left) and UK1 stratum (upper right). The two 30 × 30 km strata are ~50 km apart. Bathymetry maps are color coded by depth (m) from deepest (blues) to shallowest (reds). (For interpretation of the references to color in this figure legend, the reader is referred to the web version of this article.)

Drazen, 2009, 2011; Priede et al., 2010; Jamieson et al., 2011). Fish make up the top level of the abyssal food web (Drazen et al., 2008) and are a crucial component of a complete ecological baseline study. Because densities of these large, mobile predators and scavengers are low in the abyss (on the order of hundreds of individuals per km^2), ROV and AUV video and photo transects require large sampling efforts for gathering quantitative datasets for these animals (Trenkel et al., 2004; Milligan et al., 2016). Baited cameras are efficient at attracting and censusing these animals, though they provide only relative estimates of densities. Regardless of technique, this is the first published study to report on the fishes and bait-attending fauna of the CCZ.

While abyssal habitats in other oceans are traditionally considered to be flat plains, the abyssal region, including the CCZ in the Pacific, has long been known to be a system of undulating, valleys and ridges lower than 1000 m in height with widths of 1–10 km (Smith and Demopoulos 2003). Recent advances in gravimetry, satellite altimetry, and increased seafloor mapping efforts, have revealed that small seamounts (< 1 km), sometimes referred to as abyssal hills, and large seamounts are also common features (Yesson et al., 2011; Kim and Wessel, 2011; Harris et al., 2014). Henceforth the term 'abyssal hills' will be used to refer to 'small seamounts' that have elevations of < 1 km. The general question of how seafloor topography, especially seamounts, influences the spatial distribution of animals has been a topic of ecological research since the 50's (Hubbs, 1959). Recently, seamount research has accelerated, yet only several hundred of the thousands of seamounts in the world ocean have been sampled (Clark, 2009; Yesson et al., 2011). Although many seamount paradigms and hypotheses still need to be rigorously tested, there is evidence that seamounts can be characterized by high benthic species richness and elevated abundance and biomass (Pitcher et al., 2007; Rowden et al., 2010). Seamount communities likely experience different hydrodynamic (enhanced current velocities, turbulence, and shear), geological (enhanced substrate and slope heterogeneity), and biological (enhanced POC flux, food, and nutrient availability) forcing relative to surrounding deep-sea habitats (Genin, 2004; Carter et al., 2006; Genin and Dower, 2007; Wessel, 2007; Lavelle and Mohn, 2010; Turnewitsch et al., 2015).

Despite this paucity of sampling, the volume of published work on seamounts dwarfs that on abyssal hills. In fact, many studies have highlighted the need for more work on smaller, deeper features (eg. McClain, 2007; Pitcher et al., 2007; Rowden et al., 2010; Yesson et al., 2011). The deep-sea scientific community has only very recently begun to explore the influence of abyssal hills on megabenthic communities (Durden et al., 2015; Milligan et al., 2016). This recent work has found elevated benthic invertebrate megafaunal biomass on hills, and increased dominance by suspension feeders suggesting that hills are an important source of heterogeneity and biodiversity in abyssal ecosystems (Durden et al., 2015). The abyssal seafloor is the largest benthic habitat on the planet (Smith et al., 2008), and abyssal hills are their most common feature (Kim and Wessel, 2011; Harris et al., 2014). An understanding of the impact of these features on deep-sea communities is thus fundamental to understanding global ecosystems. Abyssal-hill research may also have implications for nodule mining because many mining claim areas are dotted with these poorly understood features, and they have been identified as important habitat to be included in the potential marine reserves in the CCZ (Wedding et al., 2013; Danovaro et al., 2017).

Here we report results from the first baited-camera deployments in the CCZ region, report on the key environmental variables that influence this community, and place the regional bait-attending community into a larger biogeographic context. We test the hypothesis that bait-attending communities change across the CCZ in response to key environmental predictors. Specifically, we test the hypotheses that 1) abyssal hills influence the megafaunal bait-attending community in the CCZ and 2) that manganese nodule cover and relative differences in depth (bathymetric position index) positively relate to the bait-attending community diversity and change species composition.

2. Methods

2.1. Study site

We collected data from three regions in the Clarion-Clipperton Zone (CCZ; Fig. 1). The CCZ is bounded by the Clarion Fracture Zone to the north and the Clipperton Fracture Zone to the south and stretches from approximately 115°W to 155°W and 5°N to 20°N (Wedding et al., 2013; Mewes et al., 2014). We include 12 baited camera deployments in the eastern CCZ region at depths ranging from 3543 m to 4291 m. Half of these deployments are from the Ocean Mineral Singapore (the OMS stratum) claim-area and the other 6 from a UKSRL (UK Seabed Resources, LTD; the UK1 stratum) claim-area (Fig. 1e, Table 1). We include one additional deployment from the northern CCZ in 'Area of Particular Environmental Interest' (APEI) 6, one of nine 400 × 400 km APEIs in the CCZ placed off-limits to mining by the ISA (Wedding et al., 2013, 2015) (Fig. 1c). These 13 deployments were conducted on the AB02 ABYSSLINE Project cruise in Feb-Mar, 2015. Finally, two additional deployments from the western CCZ were conducted during a separate cruise with the same sampling system from Aug-Sept, 2015, with one deployment at a northern station (stratum EQPAC1) and one deployment further south (stratum EQPAC2) (Fig. 1b and d, Table 1).

The CCZ is characterized by a gradient of primary production. Chlorophyll concentrations in the southern CCZ are influenced by equatorial upwelling and generally decrease to the North and to the West (data from MODIS satellite: https://oceancolor.gsfc.nasa.gov/). Average bottom temperatures are below 2 °C at all study sites. The average depth in the eastern CCZ is ~4600 m deepening to ~5200 m in the western CCZ. The general bathymetry of this region is characterized by NNE-SSW oriented, kilometers-long horst and graben structures less than 100 m in height. However, UK1 and EQPAC2 were also characterized by abyssal hills ranging from 1 to 8 km in diameter and rising to a few hundred meters in height (Fig. 1d and e).

2.2. Data collection

Deployment locations were determined randomly, except for the deployments directly on abyssal hill features (CA09, EQPA2). All study areas were entirely unmapped prior to this expedition; therefore, there was no prior knowledge of the complex bathymetry of the UK1 site when random station locations were generated. However, due to interest in the abyssal hill features, one deployment was strategically moved to be directly on the summit of one of these hills. The northern and western deployments were all gathered opportunistically and were chosen for their proximity to other sampling sites, although the EQPAC2 deployment again specifically targeted the crest of an abyssal hill feature.

All video was collected using the DeepCam, a newly designed, 6000 m rated, free-falling stereo-video lander system. It was equipped with twin acoustic releases (Teledyne Benthos 865 A) and a current meter (Nortek Aquadopp 6000) mounted upright 1.45 m above the seafloor. The HD camera pair (Canon G20 VIXIA HF G20) was geometrically-calibrated, in titanium housings, and controlled and maintained in sync through a custom designed computer and intervelometer. Cameras were mounted on an aluminum frame at a slightly downward angle (7° declination from horizontal) at 0.56 m above the seafloor, providing a 1.86 m^2 half-elliptical field of view. This allows for observations of approach behaviors as well as side views of all fauna, which aid greatly in identification. Camera geometry was calibrated, enabling accurate and precise three-dimensional measurements in the field of view (using CAL and EventMeasure software by SeaGIS). The lander was equipped with two white 3700 lm LED lights in sync with the two cameras (DSPL SeaLite Sphere SLS 3100). For every deployment, the lander was baited with ~1 kg of Pacific mackerel (*Scomber japonicus*), which is maintained in the center of the field of view 1 m in front of the cameras. Video was recorded in 2-min intervals (clips) with

Table 1
Deployment information and associated environmental variables for baited-camera deployments. Depth is ADCP recorded maximum depth. "Temp" refers to the average on-bottom temperature from the ADCP. 'Chl' refers to the 13-year, long-term average surface chlorophyll in that 30 by 30 km stratum. 'Nodule Cover' refers to the proportion of the evenly illuminated seafloor that was taken up by nodules. "Easterly" refers to the eastern component of the vector of the average ADCP current direction near the seafloor; "Northerly" is the northern component of the vector of the average current direction. 'Rugosity' refers to the vector ruggedness metric (VRM) which quantifies rugosity using the dispersion of the vectors orthogonal to the bathymetry (Sappington et al., 2007). 'Fine BPI' refers to the fine-scale bathymetric position index value. 'Broad BPI' refers to the broad scale bathymetric position index value. 'Zone' refers to the broad topographic category (flat, slope, crest, and depression) into which the deployment was placed by the Benthic Terrain Modeler (Wright et al., 2012).

Drop	Stratum	Lat	Long	Depth	Temp	Chl	Nodule Cover	Easterly	Northerly	Avg Current Sp.	Max Current Sp.	StdDev Current Sp.	Slope	Rugosity	Fine BPI	Broad BPI	Zone
		(deg)	(deg)	(m)	(C)	(g/m^3)				(m/s)	(m/s)	(m/s)	(deg)				
CA01	UK1	12.38	−116.49	4201	1.52	0.143	0.5	−0.72	0.70	0.09	0.20	0.04	2.42	5.68E−04	−43	8	flat
CA02	UK1	12.57	−116.71	4267	1.83	0.143	0.03	0.48	0.88	0.06	0.23	0.03	3.15	9.98E−04	5	−33	flat
CA03	OMS	12.12	−117.36	4244	1.57	0.146	0.36	0.63	0.78	0.06	0.18	0.03	5.17	2.03E−03	35	−65	slope
CA04	OMS	12.07	−117.18	4141	1.56	0.146	0.59	0.86	−0.51	0.04	0.17	0.02	4.59	5.33E−04	−14	12	flat
CA05	OMS	12.19	−117.33	4126	1.56	0.146	0.5	−0.85	0.52	0.04	0.13	0.02	1.13	1.80E−03	84	66	flat
CA06	UK1	12.51	−116.62	4275	1.58	0.143	0.83	1.00	0.02	0.09	0.27	0.06	2.72	5.99E−03	−14	−116	flat
CA07	UK1	12.55	−116.54	4312	1.59	0.143	0.13	1.00	0.04	0.04	0.12	0.02	1.34	2.77E−03	5	−83	flat
CA08	UK1	12.45	−116.65	4263	1.58	0.143	0.56	−0.98	0.19	0.06	0.15	0.02	1.76	1.36E−02	−4	−164	flat
CA09	UK1	12.44	−116.55	3605	1.58	0.143	0.17	−0.12	−0.99	0.04	0.15	0.02	6.51	5.75E−03	144	525	crest
CA10	OMS	12.14	−117.25	4158	1.56	0.146	0.12	−0.99	−0.13	0.04	0.18	0.02	5.64	1.58E−03	−63	−10	slope
CA11	OMS	12.05	−117.22	4153	1.56	0.146	0.5	1.00	−0.04	0.04	0.15	0.03	0.73	1.29E−03	35	−6	flat
CA12	OMS	12.03	−117.35	4156	1.56	0.146	0.3	−0.77	−0.63	0.05	0.12	0.02	2.87	1.38E−03	25	11	flat
CA13	APEI6	19.45	−120.06	4127	1.63	0.086	0.48	−0.53	−0.85	0.03	0.23	0.02	1.96	3.58E−03	−93	−41	flat
EQPAC1	EQPAC1	7.93	−154.93	5231	1.50	0.107	0	−0.50	−0.87	0.08	0.14	0.02	0.26	1.18E−03	−2	43	flat
EQPAC2	EQPAC2	5.02	−155.10	4170	1.44	0.154	0	0.89	0.45	0.05	0.21	0.03	32.29	6.27E−02	−409	811	crest

8-min rest periods to stretch battery life to 24-h and to minimize light disturbance to bait-attending fauna.

Baited traps were deployed at each station approximately 2 km away from simultaneous camera deployments to collect voucher specimens for accurate morphological and genetic identification. 2 km were chosen to maintain a safe separation between the two free vehicles while still sampling the same area and minimizing bait plume interaction. The trap was a free vehicle mesh box (2.3 mm mesh size) about 2 m^3 in volume, baited with one mackerel wrapped in mesh. The trap had six funnel-shaped entrances (4 with openings of 0.5 m^2 and 2 with openings of 0.75 m^2), and12 squid-baited hooks on the outside, as well as two mackerel-baited PVC amphipod traps (one inside and one attached to the top of the trap) each with two 2.5 cm diameter funnel openings.

2.3. Data processing

For the DeepCam videos, all visible megafauna were recorded and identified to the lowest possible taxonomic level (generally to species or genus). 'Bait attending' is used as a general term to refer to those organisms attracted to bait, gathering around bait, actively consuming bait, or preying on amphipods and other scavengers (necrophagivores). Sessile taxa (e.g., xenophyophores) and all observed benthopelagic planktonic fauna (e.g. larvaceans) were noted but not included in statistical analyses. Small scavenging amphipods were extremely abundant in all deployments, but could not be counted due to their small size. Large amphipods (> 5 cm) identified from trapped specimens to be *Eurythenes gryllus* were counted (*Eurythenes* sp.). Time of first arrival (T_{arr}) was recorded for each bait-attending taxon. The maximum number individuals within each taxon visible at one time (in a single frame) for each 2-min clip (clip-wise MaxN) was used characterize differences between regions. In addition, the maximum number of individuals of each taxon visible in one frame for each deployment (drop-wise MaxN) was used for further analyses as conservative count data for diversity calculations and community composition statistics (following Cappo et al., 2006).

Coryphaenoides spp. was the dominant taxon observed, so length measurements and mass estimations were made for individuals when possible. Pre-anal fin length (PAFL) was measured in the video from snout tip to pre-anal fin origin for at least three different frames for each individual. Measurements were only accepted if they met precision standards (RMS > 10 mm, precision to length ratio < 5%, precision < 10 mm). The mass of each measured fish was estimated using the PAFL versus mass relationship derived from trapped individuals (n = 22). Absolute abundances were estimated using a model based on time of first arrival (T_{arr}), current velocity, and fish swimming speeds while assuming a uniform distribution of fishes (Priede et al., 1990; Priede and Merrett, 1996; Supplementary Materials Eqn. 1). These estimated abundances for *Coryphaenoides* spp. are given to place the abundances in a larger biogeographic context with comparison to the literature.

Swimming speeds were measured using the stereo video and used to estimate abundances. Because the abundance models are specifically designed for rattail fishes, speeds were only estimated for *Coryphaenoides* spp. Measurements were taken by tracking the tip of a fish's snout in three-dimensional space over time. A minimum of three point measurements were taken, each spaced approximately 25 frames apart (frame rate of 29 fps). Each individual fish was tracked during its straight approach for as long as possible (3–16 s), and an average speed was calculated for each individual. Average approach speed of *Coryphaenoides* spp. measured in each of 10 deployments was used to estimate abundance using the previously mentioned model; for deployments where approach speed could not be directly measured (due to low numbers of suitable images), the overall average approach speed (0.072 m/s, range = 0.01 to 0.33) was used.

Lander heading, depth, bottom temperature, current velocity, and current direction were recorded by the current meter. Due to partial

blocking of one measurement beam by the lander frame, current velocities were calculated assuming 0 vertical velocities, a reasonable assumption for these depths (Wyrtki, 1961). Average current direction was calculated over the entire deployment using a circular mean function. This average direction vector was then converted into its two components: Northerly and Easterly.

The highest resolution bathymetry available (50 m for the eastern CCZ, 85 m in the north, 70 m in the west) was used to derive all topographic predictors for each deployment using the spatial analyst tools and the Benthic Terrain Modeler (BTM) for ArcGIS 10.0 (Wright et al., 2012). The Benthic Terrain Modeler is a collection of GIS tools that calculates slope, rugosity, and broad and fine-scale bathymetric position indices (BPI) for bathymetric grids; it also classifies the grid into terrain types based on these criteria. Topographic predictors included in our analysis are fine and broad-scale bathymetric position index values (BPI), slope, aspect, and curvature. BPI is a continuous metric that combines absolute depth, the depths of a specified neighborhood, and calculated slopes to provide a relative depth metric for each point in a bathymetric grid (see Supplementary Table 1 for precise definitions). BPI scales were chosen to reflect the data resolution and the size of the abyssal hills that were characteristic of this dataset. Therefore, the fine scale BPI used an inner radius of 1 cell size (50–85 m depending on resolution) and an outer range of ~500 m (about 10 cells around each center). The broad-scale BPI scale was set to ~2.5–5 km reflecting the range of diameters of the abyssal hills. Additionally, habitat complexity was quantified on two scales using the Vector Ruggedness Metric (VRM) (Suppl. Table 1). The two chosen scales reflected the broad and fine BPI scales, 500 m and 2.5 km.

Average productivity was calculated for each deployment using chlorophyll-a data derived from AQUA MODIS satellite data (http://coastwatch.pfeg.noaa.gov/erddap/index.html). We used an average value over the entire timespan of the MODIS dataset (January 2003 to January 2015) for a 30 km by 30 km box centered around each deployment location. Average chlorophyll was also calculated for the year and for the month preceding each deployment to include various timescales of export. However, only the long-term chlorophyll was included in the reported statistical models because the results were similar independent of which timescale of chlorophyll was used in the models.

Percent nodule cover was also estimated for each deployment using the subsection of the field of view with the most consistent lighting. Proportion of nodule cover was derived from a spectral analysis of images of the subsample section by identifying dark pixels as 'nodule' and light pixels as 'sediment' using an online image color extractor (http://www.coolphptools.com/color_extract). The results were corroborated by visual estimates.

2.4. Statistical analyses

The influence of abyssal hills, nodule cover, and the other environmental parameters on the bait-attending community were tested with statistical models with varying response variables but identical environmental predictors and similar evaluation procedures using the programming language R (R Core Team, 2015). Model structure (i.e. distributions used) was chosen based on an analysis of the response variable and behavior of residuals (deviance residuals). A beta-regression model was used to evaluate diversity (based on drop-wise MaxN), and generalized linear mixed models (GLMMs) (as in Jackson et al., 2012) were used to evaluate changes in and influences on community composition. A generalized linear model was used to evaluate oceanographic and topographic impacts on *Coryphaenoides* spp. length. For each model, deviance residuals were assessed for distribution assumption, constant variance, outliers, and shape assumptions (i.e. patterning in residuals plotted against each predictor).

The initial set of environmental predictors included both topographic and oceanographic variables as discussed above (Table 1). Due to the limited number of deployments (n = 15) and to reduce issues of multicollinearity, the number of predictors for the starting models were reduced by eliminating those that were highly correlated via analysis of pairwise Pearson correlation ($r > 0.80$). As a result, depth and slope (highly correlated with both fine-scale and broad-scale BPI), and rugosity on the scale of 500 m (highly correlated with fine-scale BPI) were removed from the starting models. Larger scale rugosity (at a scale of 2.5 km) was also correlated with fine-scale BPI ($r = 0.86$) and with broad-scale BPI ($r = 0.77$); however, because the effect of rugosity was of interest, the larger scale rugosity predictor was retained in the starting models. This elimination resulted in a starting model with 11 predictors: maximum current speed, average current speed, standard deviation of current speed, average direction of the current (easterly and northerly components of average current directionality separate), large scale rugosity, average surface chlorophyll, average bottom temperature, broad-scale BPI, fine-scale BPI, and proportion nodule cover.

These predictors were further reduced for each model individually using an iterative variance inflation factor (VIF) procedure with a threshold of 3, where the predictor with the highest VIF was sequentially removed until all values were below 3 as recommended by Zuur et al. (2010) (Barton, 2016). This was done to minimize collinearity in the predictors for each model. The best model(s) was then selected by comparing all possible model combinations on the basis of Akaike Information Criterion (AICc) scores and r^2values (Barton, 2016). For equivalent models (those with AICc values within 2 units of each other and equal r^2 values), all results were reported (Supplementary Tables). Model performance was evaluated through visual examinations of deviance residuals for possible outliers as well as deviations from normality and/or uniformity (e.g. Zuur et al., 2010). This methodology was applied to each of the models described below.

We evaluated topographic and oceanographic predictors influence on **community diversity** (Simpson index of diversity) using a beta-regression model with a log link function (Cribari-Neto and Zeileis, 2010). First the diversity index was calculated using the drop-wise MaxN of each taxon for each deployment. The Simpson Index of Diversity (1-D) was chosen because it is more sensitive to changes in the most common species, so results would be less likely to be skewed by rare species. Shannon-Wiener Diversity Index was also calculated and was found to be highly correlated ($r^2 = 0.88$) with Simpson Index values. Because the Simpson Index ranges from 0 to 1, a beta regression model was used to evaluate topographic and oceanographic drivers of diversity patterns (Cribari-Neto and Zeileis, 2010). A beta regression is essentially a generalized linear model which assumes a beta distribution (as opposed to Poisson, Gaussian, etc.) and can successfully model continuous data on the 0–1 interval (Cribari-Neto and Zeileis, 2010). Moreover, the four different regions were also compared using species richness by pooling deployments from each stratum to calculate estimated species richnesses with rarefaction, although only the two mining claim areas had large enough sample sizes to calculate ES100 (Oksanen et al., 2015). ES14 was used to compare all 5 strata. Additionally, species accumulation curves and estimated species richnesses were compared for the UK1 and OMS strata, and estimated total species richness for the two strata were evaluated with both the Chao I estimate and a bootstrapping estimate (Oksanen et al., 2015). Mean species richness and diversity was compared among the different regions in this study and among published baited camera data from the Californian slope (Yeh and Drazen, 2011), the Hawaiian Islands (Oahu) and the Northwestern Hawaiian Islands (Laysan Island, Pearl and Hermes Atoll; Yeh and Drazen, 2009), and from the Southwestern Pacific (Kermadec Trench; Jamieson et al., 2011) with an ANOVA and a Tukey HSD posthoc test to give a biogeographic comparison.

Topographic and oceanographic influences on **community composition** were investigated with mixed-effects models (GLMMs) using drop-wise MaxN as the response and random effects by species for each predictor (Bates et al., 2015). A Poisson distribution was used for the

model with a log link function. BPI, temperature, average current speed, and Northerly were all standardized to a mean of 0 for the GLMM as suggested by Jackson et al. (2012). After using VIF to reduce the number of predictors of the generalized linear models, all possible model combinations were tested and ranked using AICc (Saefken et al., 2014; Barton, 2016). The resulting 'top' models were then explored for evidence of possible community composition changes across gradients of environmental predictors using random effects. Random effects by species were added for all predictors included in at least one of the top models as in Jackson et al. (2012), and all possible mixed model combinations were evaluated and ranked with AICc to identify the final 'best' model. Note that models which included a random effect for a predictor but which did not also include the fixed effect of that predictor were not included in the model rankings. AICc-equivalent (within 2 AICc points of each other) top ranked models were all reported (Supplementary Table 2). Random effects allow the regression coefficients (slope & intercept) to vary among species, thus detecting predictors which result in species-specific differences, and therefore identifying those predictors which drive changes in community composition (Jackson et al., 2012). Note that in contrast, fixed effects fit the same slope for all species and allow only the intercepts to vary among species. Employing mixed models to analyze changes in community composition in this way has proven valuable in separating composition vs. abundance changes as well as handling collinearity among predictors (Jackson et al., 2012). Evaluation of the significance of each random effect in the best model was done with a two-step process: firstly, the change in the AICc (dAIC) of the model due to the addition of the random effect had to be > -2, indicating a significant increase in explained variation given the added complexity of the model. Secondly, an ANOVA comparing a model with the random effect to a null model without the random effect had to show a significant difference between the two ($p < 0.05$). Those random effects which passed both tests were reported to be causing significant changes in community composition across deployments.

To address changes in **biomass** of *Coryphaenoides* spp., across environmental predictors, we used a GLM. Mass could only be estimated for the dominant predator and scavenger *Coryphaenoides* spp., the only taxa for which sufficient images and physical trapped specimens were available. A Kruskal-Wallis nonparametric means comparison with a Dunn post-hoc test with a Bonferroni correction was used to test for differences in pre-anal fin length (PAFL) and mass between strata. To understand which variables caused strata-differences in size, a gamma GLM was used to evaluate the influence of topographic and oceanographic variables on PAFL and mass of the dominant scavenger.

Finally, in order to place our results in a broader biogeographic context, we conducted a small review of recent baited camera work in the Pacific in order to compare the diversity and MaxN of the CCZ to those recorded from Hawaii, the Californian margin, and the SW Pacific using ANOVA with a Tukey HSD post hoc test. Abundances from this dataset (Table 2) are compared to other baited camera studies using MaxN. For *Coryphaenoides* spp. estimated densities are also presented (Table 4) as calculated from the Priede et al. time-of-first-arrival (T_{arr}) method (Supplementary Materials Eqn. 1) created specifically for rattail fishes (Priede et al., 1990; Priede and Merrett, 1996).

3. Results

3.1. General megafaunal assessment

Twenty-three morphotypes from six different phyla were observed over 15 baited camera deployments (Fig. 2). Fifteen of these 23 were deemed "bait-attending") and are examined in this study (Table 2). The dominant taxa were *Coryphaenoides* spp., *Hymenopenaeus nereus*, and *Plesiopenaeus armatus*. Additionally, large numbers of small amphipods were observed but could not be identified or quantified. The larger amphipods were clearly visible and identified from trap specimens as *Eurythenes gryllus*. Three morphotypes of zoarcids were defined: *Pachycara nazca* (Fig. 2k) identified from trapped specimens; zoarcid sp. 1 (Fig. 2n) which was very small, frequently curled up, and had a short,

Table 2
Deployment MaxN for each bait-attending species by camera deployment. Note *Eurythenes* sp. refers to the large individuals that could be identified and counted from the camera data. The bottom row gives the sum of the MaxNs for each species.

						Fish									Decapods			Other			
Drop	Stratum	Zone	Latitude	Longitude	Depth	*Barathrites iris*	*Bassozetus* sp.	*Bathyonus caudalis*	*Coryphaenoides* spp.	*Histiobranchus bathybius*	Ophidiidae sp.1	*Pachycara nazca*	Zoarcidae sp.1	Zoarcidae sp.2	*Plesiopenaeus armatus*	*Hymenopenaeus nereus*	*Munidopsis* sp.	*Eurythenes* sp.	*Ophiomusium* cf. *glabrum*	*Plesiodiadema* sp.	Grand Total
CA01	UK1	flat	12.38	-116.49	4201		1		6	1		2			5	2			2	1	20
CA02	UK1	flat	12.57	-116.71	4267		1		5						6	9		1			22
CA06	UK1	flat	12.51	-116.62	4275	1	1	1	7			1			4	3			2		20
CA07	UK1	flat	12.55	-116.54	4312		1	1	8					1	9	8		1			29
CA08	UK1	flat	12.45	-116.65	4263		1		5	1			1		6	5			1	1	21
CA09	UK1	crest	12.44	-116.55	3605			1	7		1	3	1		3	8	1			15	40
CA03	OMS1	slope	12.12	-117.36	4244				8						5	6			2		21
CA04	OMS1	flat	12.07	-117.18	4141		1	1	3	1					3	4			1	7	21
CA05	OMS1	flat	12.19	-117.33	4126		1		8			1		2	3	9			3	8	35
CA10	OMS1	slope	12.14	-117.25	4158				2			2			3	6			2		15
CA11	OMS1	flat	12.05	-117.22	4153		2		7			1			3	5			2	5	25
CA12	OMS1	flat	12.03	-117.35	4156				2			1			3	9			2	1	18
CA13	APEI4	flat	19.45	-120.06	4127				5						3	6			1		15
EQPAC_CA01	EQPAC1	flat	7.93	-154.93	5231	1	3		5						3	1		1			14
EQPAC_CA02	EQPAC2	crest	5.02	-155.1	4170	2	7		5						17	1		1			33
						4	**19**	**4**	**83**	**3**	**1**	**11**	**2**	**3**	**76**	**82**	**1**	**4**	**18**	**38**	**349**

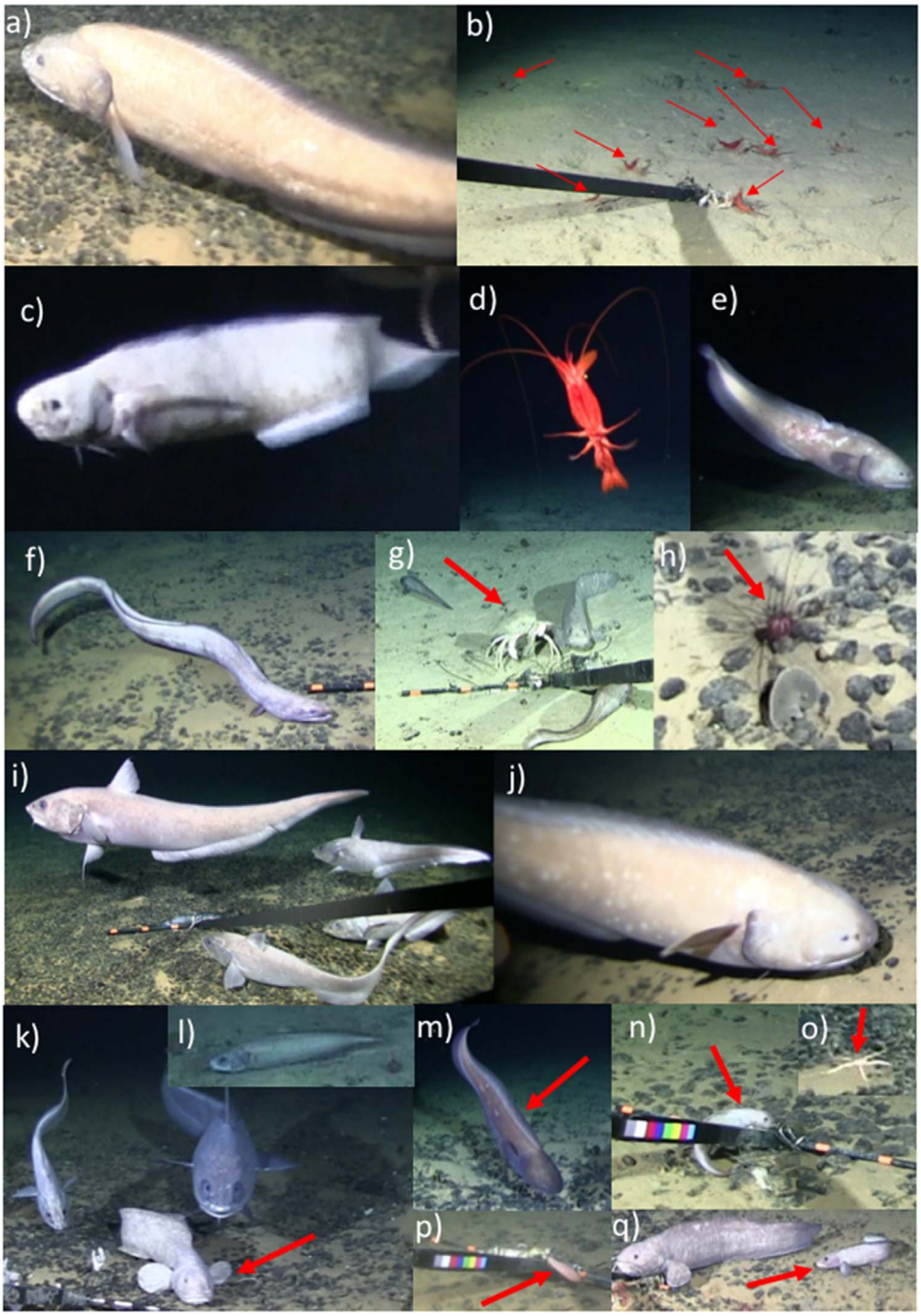

Fig. 2. Representative photographs of observed putative bait-attending species. a) *Bathyonus caudalis* b) group of *Hymenopenaeus nereus* c) *Barathrites iris* d) *Plesiopenaeus armatus* e) *Bassozetus* sp. f) *Histiobranchus bathybius* g) *Munidopsis* sp. (arrow) and three zoarcids including *Pachycara nazca* h) *Plesiodiadema* sp. (arrow) and plate like Xenophyophore i) *Coryphaenoides* spp. j) *Bassozetus* sp. light morphotype k) *Pachcara nazca* (arrow) and two *Coryphaenoides* spp. (above) l) unidentified Ophidiidae sp. 1 m) *Bassozetus* sp. dark color morph (arrow) n) unidentified zoarcid species, Zoarcidae sp. 1 o) *Ophiomusium* cf. *glabrum* p) large *Eurythenes gryllus* q) unidentified zoarcid species, Zoarcidae sp. 2 (arrow) with *Pachycara nazca*.

bluntly rounded head; and zoarcid sp. 2 (Fig. 2q) which was generally of intermediate size with dark fin edges and a narrow, tapered head. Although it has been suggested that differences in light reflection off scales can be used to distinguish between *C. armatus* and *C. yaquinae* despite the inadequacy of image-specific morphometric features, we have found that for our camera system, color and reflection tend to vary with distance and angle to the cameras (Jamieson et al., 2012). Therefore, to avoid misidentifications, *C. armatus* and *C. yaquinae* were not identified to species in our dataset. The baited traps captured both species, though only one of 22 was confirmed to be *C. armatus* both morphologically and genetically (M. Gaither unpubl).

Of 15 bait-attending putative species, 8 were found only on flat terrain and two were found only on abyssal hills ("crest" or "slope" zones as defined by BTM; Table 2). Across study locations, the greatest contrasts were seen between the western and eastern CCZ, with no zoarcids, much lower numbers of the small shrimp *H. nereus,* and much higher numbers of the ophidiids *Barathrites iris* and *Bassozetus* sp., in the west (Fig. 3). The ophidiids were recorded more consistently in the western regions; they were observed in a higher proportion of clips per deployment in the west than in either the east or the north (Suppl. Fig. 1). The dominant scavengers, *Coryphaenoides* spp., also showed regional variations. The average deployment MaxN of *Coryphaenoides*

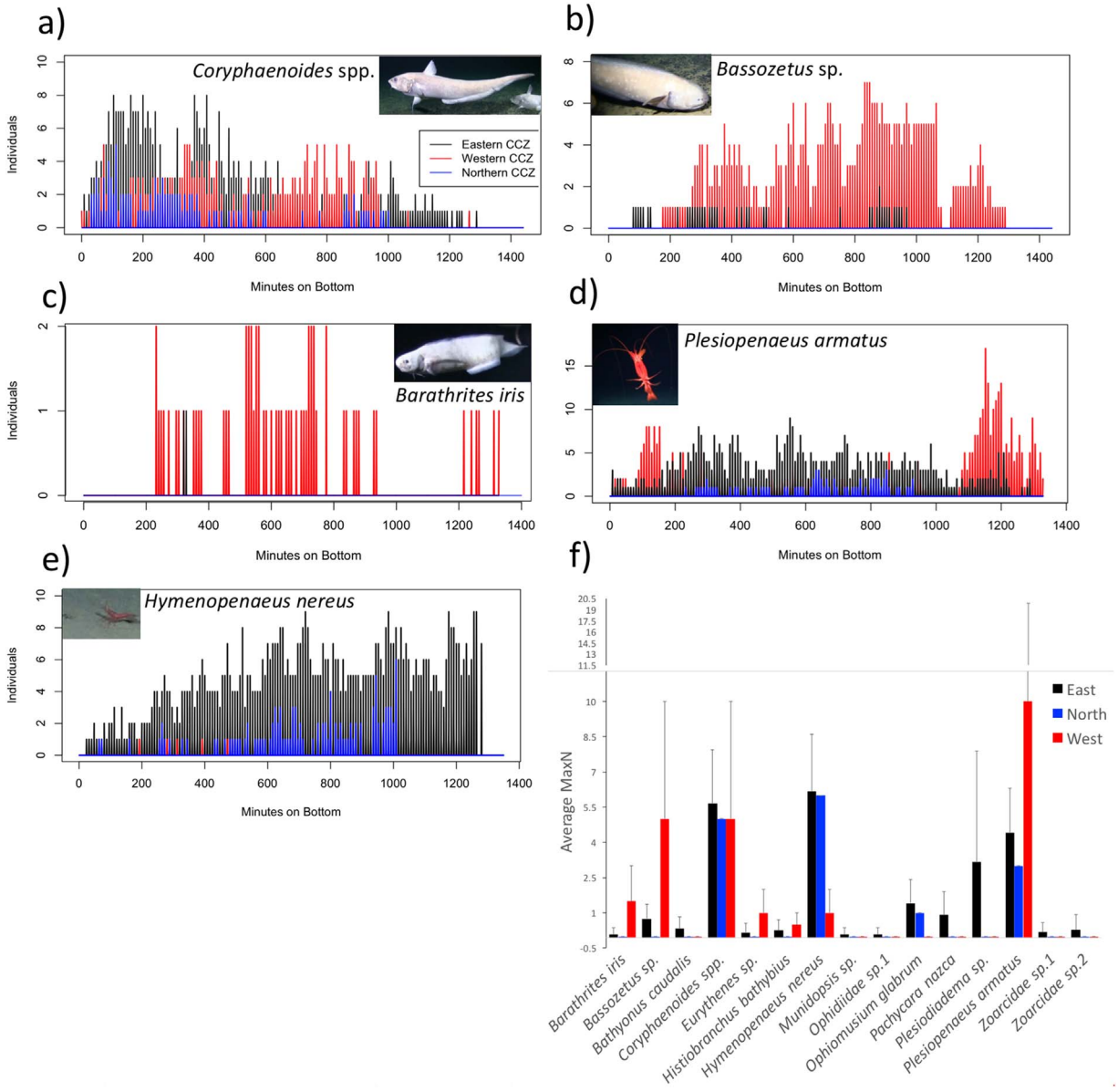

Fig. 3. Differences in the presence of 5 important putative species across the three geographic regions sampled in this study. Each graph in panels a-e presents averages of clip-wise MaxN's (per 2 min video clip) for deployments pooled by region i.e. each bar represents the mean across all deployments in a region at that bottom time. Sample sizes for the eastern, northern, and western regions are 12, 1, and 2 respectively f) The average drop-wise MaxN (per deployment) for all putative species in all three regions with standard deviations represented with error bars.

spp. was slightly higher in the east than in the west (Fig. 3f), and the presence characteristics (e.g., clip-wise MaxN) showed obvious regional differences (Fig. 3a). *Coryphaenoides* spp. was present consistently at high numbers for the majority of a deployment in the east, while in the west and north the numbers were generally lower throughout a deployment (Fig. 3a and Suppl. Fig. 1). *Plesiopenaeus armatus* also showed marked differences in the east versus the west, arriving earlier in the west but generally remaining at low numbers until the end of the deployment, when they vastly outnumbered all other taxa (Fig. 3d). Their average deployment MaxN in the west was more than double that in either the east or the north (Fig. 3e).

Rarefaction curves showed that the eastern CCZ had the highest species richness, followed by the western and the northern CCZ. The greatest common expected species count possible (ES14) for all strata was: UK1 = 6.1, OMS = 6.0, EQPAC1 = 5.8, EQPAC2 = 4.8, APEI = 3.9. Within the eastern region, estimated species richness was highest in the abyssal hills stratum of UK1 (ES100 = 13); however, only the UK1 and OMS strata had sufficient sampling to estimate an ES100 (Fig. 4a). Moreover, only OMS seems to have been sufficiently sampled with the number of species approaching an asymptote at an estimated species richness of 9, while the UK1 curve continues to rise with an estimated species richness of 15 (Fig. 4a). The estimated number of species at UK1 was higher than at OMS regardless of the estimation method used (Chao: 17.2 ± 2.97 vs. 12.5 ± 3.79; Bootstrap: 16.7 ± 1.31 vs. 11.0 ± 1.05).

3.2. Abundance and size of Coryphaenoides spp.

T_{arr}-derived abundances had a range from 12 to 47,834 individuals per km^2, giving an estimated average of 4891 per km^2 across the whole CCZ. Removing the two deployments with a T_{arr} of less than 5 min reduces the range to 12–1530 individuals per km2 with an average of 358 per km^2. The MaxN metric ranged from 2 to 8 and was not strongly correlated with the T_{arr} abundances (r = 0.2), and there were no significant differences in *Coryphaenoides* spp. abundance between UK1 and OMS for either metric (*t*-test, $p > 0.05$).

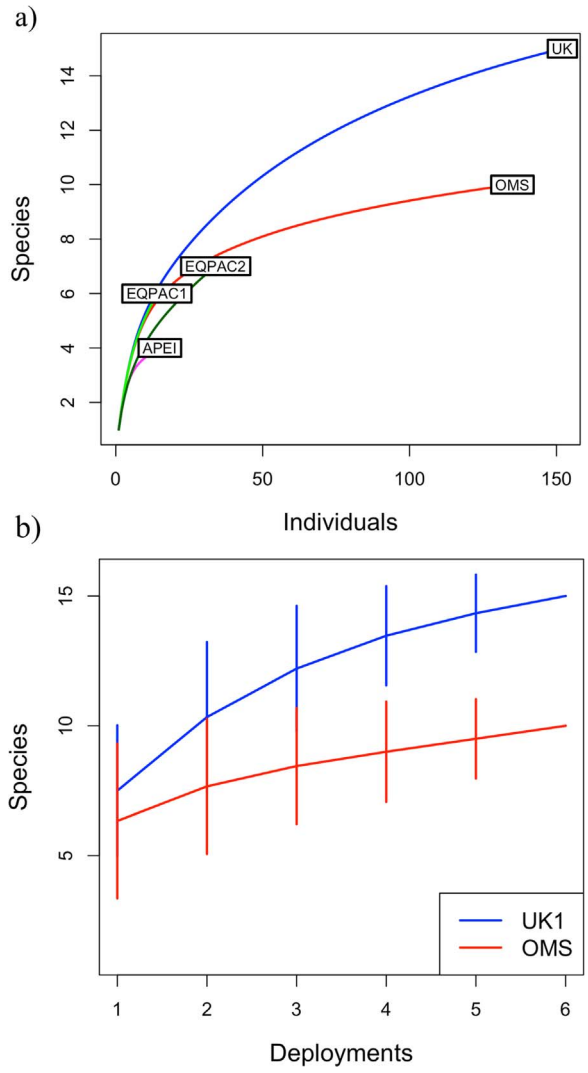

Fig. 4. a) The rarefaction curves for each sampling stratum. b) Mean species accumulation for UK1 (blue) and OMS (red) with standard deviation from 9999 random permutations of the data (Gotelli and Colwell 2001). (For interpretation of the references to color in this figure legend, the reader is referred to the web version of this article.)

PAFL of *Coryphaenoides* spp. was larger in the hills-influenced UK1 stratum (266 ± 56 mm) than in the flat OMS stratum (231 ± 59 mm *t*-test $p < 0.001$, Fig. 6). In the western CCZ the abyssal hill deployment also had significantly larger individuals than the abyssal plain deployment (Fig. 6). In testing these relationships further with a GLM, *Coryphaenoides* spp. mean length showed a significant positive correlation with broad-scale BPI (slope = 0.001, $p < 0.0001$) (Fig. 5a). Additionally, length was also positively related to bottom temperature and nodule cover (slope 1.67 $p < 0.0001$; slope = 0.52 $p < 0.0001$). Current direction was also related to PAFL, with smaller sizes found at locations with a more easterly and less northerly average current direction (slope = 0.05 $p < 0.001$, slope = −0.08 $p < 0.0001$; Fig. 5a, Supplementary Table 3). Mass of *Coryphaenoides* spp. were also greater in UK1 than OMS (mean = 2.0 ± 1.4 kg; mean = 1.4 ± 1.4 kg, *t*-test $p < 0.001$), and the generalized linear model was identical to the length model (mass(g) $= 54.347e^{0.0127PAFL(cm)}$, $R^2 = 0.87$) (Suppl. Table 3).

3.3. Diversity

The bait-attending community of the western CCZ had an average Simpson (Shannon) Diversity Index value of 0.70(1.4); the eastern CCZ had an average of 0.77(1.6), and the northern deployment had a value of 0.68(1.2) respectively (Fig. 7). A categorical comparison of diversity between strata and another between on/off hill sites (using the 'crest' classification from the benthic terrain modeler; Table 1) found no significant differences (both ANOVA $p > 0.05$). However, using continuous metrics, diversity was significantly, positively related to fine-scale BPI, nodule cover, and temperature ($p < 0.05$; Fig. 5b; Table 1). All 6 AICc equivalent diversity models included percent nodule cover and fine-scale BPI, with percent nodule cover and BPI significant in 5 of 6 the models ($p < 0.05$). Nodule cover and fine-scale BPI explained a large portion of the variability ($R^2 = 0.42 - 0.57$).

3.4. Community composition

Topography and current predictors were found to have significant effects on scavenger MaxN and community composition with GLMMs (Table 3; Fig. 5c). The initial iterative VIF process resulted in a GLM of scavenger MaxN that included average and maximum current speed, current direction (both Easterly and Northerly), average chlorophyll, temperature, and broad-scale BPI as predictors (Supplementary Table 3). After comparing all possible combinations of these fixed effects, 9 AICc equivalent 'top models' resulted, all including broad-scale BPI (Supplementary Table 3). Fifteen AICc equivalent 'best' mixed models resulted after the addition of random effects to the 'top' model (Supplementary Tables 2 and 3). Results for fixed and random effects in a mixed model each have different interpretations. For those predictors where trend lines for all scavengers are parallel, varying only in their intercepts (i.e. Fig. 5c iii and iv), there was a significant fixed effect but not a significant random effect (since all the curves are nearly equivalent), meaning there is a similar trend for all species. For predictors where the slopes of the curves vary by species, there is a significant random effect (i.e. Fig. 5c i and ii) which means species have varying responses to the predictor. This predictor is therefore causing compositional changes in the community.

Topography (broad-scale BPI) and current direction (Northerly) consistently had significant positive effects across all taxa (+0.18 $p < 0.05$, +0.18 $p < 0.01$). Average current speed had a significant fixed effect only when included without its random effect (−0.14; p value ranged from 0.02 to 0.22, Supplementary Table 3). Therefore, across all scavengers, MaxNs generally increased with more positive broad-scale BPI values and in areas with a slower, more northerly average currents (Fig. 5c i and iii). Categorically, currents were not significantly higher or more variable on/off hills (ANOVA, $p > 0.05$) over the 24-h deployment intervals.

Although MaxNs of all bait-attending taxa generally increased on abyssal hills, the effect of BPI on MaxN varied in magnitude across the different scavenger taxa suggesting changes in community composition (Fig. 5c). The most frequently included random effects in the best models were BPI, average current speed, temperature, and current direction (Easterly) (Supplementary Table 2). The random effects of broad-scale BPI and average current speed were significant as determined by AICc changes and comparisons between models with random effects and models without (dAIC = 5, ANOVA $p < 0.05$). For temperature, the random effect did significantly improve the model (dAIC = 4), but the model was only marginally different than the null (ANOVA $p < 0.1$). Therefore, we conclude that changes in community composition as seen by shifts in the relative abundances for different bait-attending taxa are in response to changes in BPI and perhaps temperature.

Across all the community models, the taxa most sensitive to changes in broad-scale BPI were: *Plesiodiadema* sp., *Bassozetus* sp., *Hymenopenaeus nereus*, and *Coryphaenoides* spp. (in decreasing order). On elevated topography with increasingly positive BPI values, community composition changed as numerical dominance shifted from *H. nereus*, *Coryphaenoides* spp., and *P. armatus* to *Plesiodiadema* sp. For *Plesiodiadema* measured MaxN doubled over the range of BPI values.

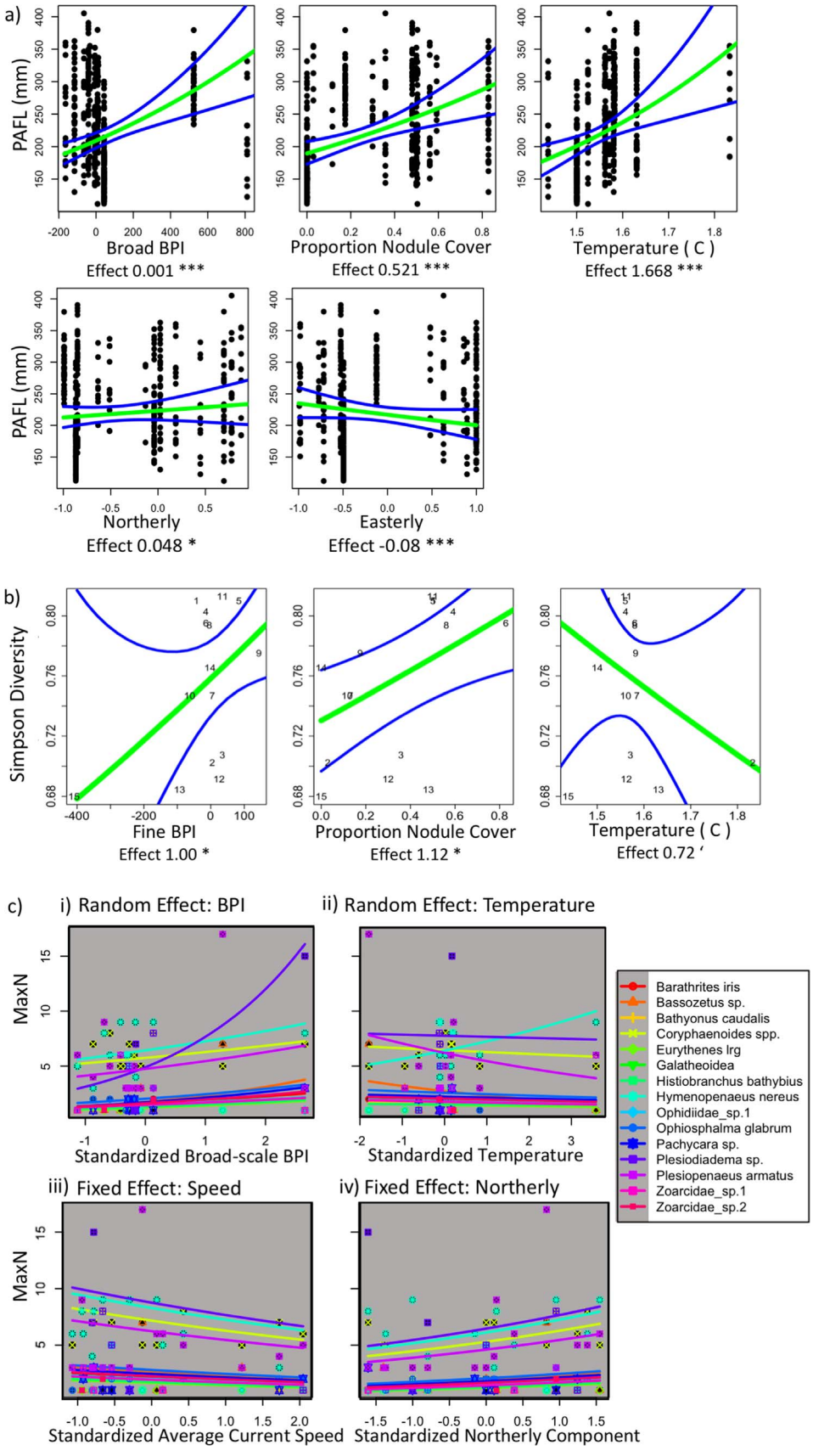

(caption on next page)

Fig. 5. Summary of the best-model results for each hypothesis. Points represent raw data. Plotted model effects are estimated by holding all other predictor values constant at their mean values. Subtitles (a, b) show magnitude of the effect and significance of each: ‘p > 0.1; *p < 0.05; ***p < 0.001. a) The effects of broad-scale BPI, nodule cover, temperature, the northerly and easterly components of the current direction (Northerly and Easterly resp.) on Pre-Anal Fin Length (**PAFL**) of *Coryphaenoides* spp. Blue lines represent 95% confidence intervals b) The effects of fine-scale benthic position index (BPI), proportion nodule cover, and temperature on scavenger *diversity* from beta-regression. Blue lines represent one standard error around each predicted value as estimated by bootstrapping (R = 9999). c) Changes of relative *abundance* (MaxN) for each species with BPI, temperature, average current speed, and Northerly all standardized to mean = 0. The equations for each of the regressions for each species for both random effects (BPI and temperature) are given in Supplementary Table 4. (For interpretation of the references to color in this figure legend, the reader is referred to the web version of this article.)

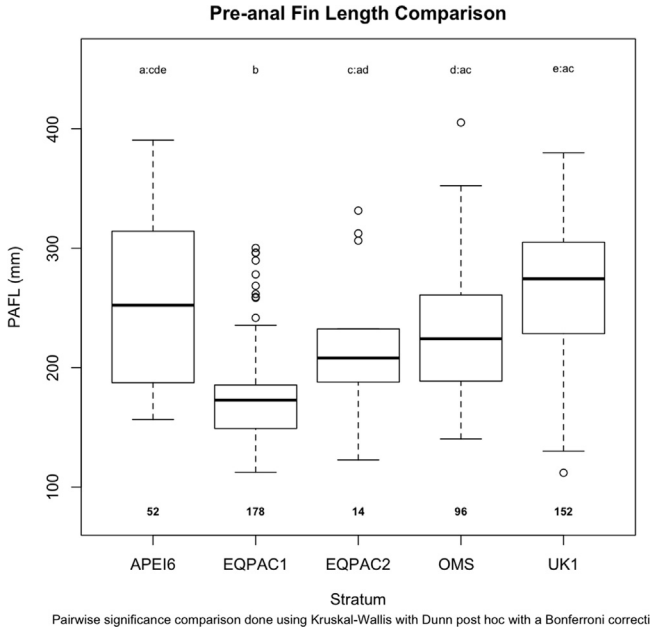

Fig. 6. Comparison of *Coryphaenoides* spp. pre-anal fin length by stratum. The box hinges represent the first and third quartiles, and the whiskers represent the 95% confidence intervals. Bolded text shows the sample sizes for each stratum. Letters above each stratum box denote significant differences between means of the strata as determined by a Kruskal-Wallis nonparametric means comparison and a Dunn post-hoc test with a Bonferroni correction. Strata are lettered in order a-e from APEI6 to UK1, and subsequent letters represent those strata which have statistically similar means as the stratum represented by the leading letter. For example, a:cde denotes that the mean length in the APEI6 stratum is statistically indistinguishable from the mean lengths of fish in EQPAC2, OMS1, and UK1 but is significantly different from the mean lengths in EQPAC1.

Bassozetus sp. also showed a similar trend. The effects of BPI on MaxN were generally small for most taxa, but even modest increases in MaxN can result in a doubling of the relative abundance for a taxa because of the low abundances seen in the CCZ.

Shifts in relative abundance in response to varying bottom temperature were also evident as seen by the differences in sign and magnitude of the scavenger responses (Fig. 5c). MaxN of *H. nereus* increased with increasing temperature unlike the other taxa. *P. armatus* and *Bassozetus* sp. showed the strongest negative MaxN trends across the temperature gradient. The other taxa seemed to have little or no response to changing bottom temperature.

Therefore, broad-scale BPI, current directionality, and average current speed each significantly impacted relative abundances (Fig. 5c, all trends move with a similar overall pattern for all species). Different species showed varying sensitivities in response to bottom temperatures and BPI, causing changes in community composition (Fig. 5c, crossing trend lines across species).

4. Discussion

4.1. Patterns in size and abundance of dominant scavenger Coryphaenoides spp

Our results suggest that there is a complex interaction between topographic and oceanographic predictors that influence the size distribution of the dominant predators, *Coryphaenoides* spp. Abyssal hills may be preferred habitat for larger *Coryphaenoides* spp. This length-topography pattern was found both at the scale of individual deployments using BPI as a continuous metric, and at the larger scale of strata: UK1 with its abyssal hills had larger fish on average than the flat OMS stratum, although the two are only ~50 km apart at their closest points (Fig. 1). *Coryphaenoides* spp. length was also significantly related to temperature, nodule cover, and current direction but, surprisingly, not to surface chlorophyll. Abyssal food availability is determined both by surface productivity and seafloor depth because the amount of carbon arriving at the seafloor declines exponentially with depth (Lutz et al., 2007; Smith et al., 2008). The bathymetric highs rather than overlying surface productivity could influence benthic food availability at the scales studied here due to less particulate organic carbon loss during sinking (likely a small effect at abyssal depths for changes of several hundred meters) or by enhancing flow and food flux to suspension feeders.

Our results show that on average, larger *Coryphaenoides* spp. are more common on small-scale bathymetric highs, and Durden et al. (2015) found significantly higher megafaunal biomass at hill sites versus plain sites in the abyssal North Atlantic. If this effectively

Table 3
A summary of the three statistical models that assessed the relationship between topographic/environmental factors and community metrics. The models consistently identified BPI, either fine-scale or broad-scale, as an important factor explaining variability of scavenger diversity, community composition, and length (for *Coryphaenoides* spp.). Note that absolute depth was considered was but highly collinear with BPI and thus removed. If included instead of BPI, it was never found to be significant. Nodule abundance, quantified as proportion nodule cover, was a significant factor in all models except the community composition model. Current direction and bottom temperature were also identified multiple times across the suite of models. The Best-fit Model column lists all the environmental predictor variables which were included in the final model along with significance: p > 0.1, ‘ 0.05 < p < 0.1; * p < 0.05; ** p < 0.01, ***p < 0.001. R^2 value for GLMM are in the form marginal; conditional.

Hypothesis	Model Response	Best-fit Model	Model Type	P	adj R^2	N
Size						
	PAFL of *Coryphaenoides* spp.	Broad-scale BPI***, Easterly***, Nodule Cover ***, Northerly*, Temperature***	GLM (Gamma, link = log)	***	0.40	490
Diversity						
	Simpson Diversity	Fine-scale BPI**, Nodule Cover*, Temperature	Beta Regression model	**	0.57	15
Community Composition						
	Species-Specific MaxN	Broad-scale BPI*, RE of BPI*, Easterly, RE of Easterly, Mean Current Speed, RE of current speed*, Northerly**, Temperature, RE of Temperature'	GLMM	***	0.067; 0.59	100

translates to higher food availability for scavengers and top predators, then abyssal hills and deep-seamounts could be preferred habitat for these animals. In addition, larger fish could be driving smaller individuals out of the prime abyssal-hills habitat. In fact, larger individuals were repeatedly observed controlling bait feeding by pushing and chasing smaller individuals. It is worth noting that differences in diet with size have been published for *C. armatus* such that larger individuals feed more heavily on carrion and benthopelagic prey than smaller individuals (Pearcy and Ambler, 1974; Drazen et al., 2008); however, these prey items have not yet been shown to be more abundant over hills. Overall, deep-seamounts seem to have a higher biomass for some taxa than abyssal plain environments; however, the biological reasons behind this relationship are not yet clear.

The significant positive relationship between *Coryphaenoides* spp. length and nodule cover could be driven by competition for prime habitat as well. For example, Vanreusel et al. (2016) found that epibenthic megafaunal densities were more than two times greater in areas of dense nodule coverage versus nodule free areas, and within the UK1 Claim Area, Amon et al. (2016) found significant correlations between the abundance of megafauna and nodule abundance. Although epifauna appear to be infrequent prey items of scavengers, diet studies for genus *Coryphaenoides* have not been conducted in regions of high nodule cover, and these fish do generally feed across the sediment surface. Therefore, if nodules act to increase epifaunal cover, then nodules could increase prey availability for the fish (Pearcy and Ambler, 1974; Drazen, 2002). Nevertheless, the linking mechanism is not clear. Though nodule abundances were not strongly correlated with any bathymetric predictor in our data, smaller-scale nodule heterogeneity has been correlated to differences in sedimentation rates, and abyssal hills have been shown to influence bottom current characteristics influencing sediment deposition and composition in the deep sea (Mewes et al., 2014; Turnewitsch et al., 2015).

Much uncertainty still exists in the abundance estimates for highly mobile megafauna, even for the most well studied abyssal example, *Coryphaenoides*. This is easily seen when comparing the large ranges of abundance estimates across the deployments (Table 1). Animal densities are a key component of ecological baseline surveys of a region (Wedding et al., 2013, 2015), and assessing the impact of mining activities on the top predators of the CCZ will depend on accurate density estimations. Though relative abundances (such as MaxN) can be compared and used for this purpose, it remains important to continue working towards a more precise and accurate method to estimate true population densities for these animals. It seems likely that large-scale, higher resolution imaging surveys (e.g., with AUVs or ROVs) will be needed to provide ground-truthing of baited-camera estimates of top-predator abundances in the CCZ.

4.2. Environmental effects on the bait-attending community: abundances, diversity, community composition

Bottom current characteristics influence baited-camera abundance estimates because bait-attending fauna generally locate carrion by tracking odor plumes spread by currents (Sainte-Marie and Hargrave, 1987; Bailey et al., 2007b). The significant effect of current speed may be due to subsequent changes in the characteristics of the bait plume, which is of obvious significance to the attraction of scavengers as noted throughout the literature (Sainte-Marie and Hargrave, 1987; Priede et al., 1990). The decrease in scavenger MaxNs with higher current speeds was surprising, since higher current speeds might be expected to increase the area of influence. However, this negative relationship could be due to more rapid dilution of the odor plume at higher current speeds, or reduced ability of scavengers to swim against currents.

Current characteristics in the CCZ may be influenced by topography in the CCZ. The general CCZ bathymetry is characterized by roughly North-South running horst and graben features, and the abyssal hills and seamounts in the region often also run along these lines (Fig. 1d). Therefore, the topography may interact differently with more northerly bottom currents, with flow steered through grabens and along the sides of abyssal-hill features. Many studies suggest changes in currents around seamounts and current steering by topography drive the higher biomass, abundance, and diversity recorded at seamounts (Pitcher et al., 2007). However, these studies are chiefly concerned with the magnitude and variability of the current (Genin et al., 1986; Carter et al., 2006; Turnewitsch et al., 2015). Although currents were not significantly higher or more variable on/off hills, current direction was significant only when included together with BPI. Therefore, the importance of current direction in our models may reflect an interaction of bottom currents with the longitudinal topography in addition to the current's direct effects on bait-attending fauna.

Nodule cover seems to have a positive influence on scavenger diversity as well as *Coryphaenoides* spp. size as discussed above. Amon et al. (2016) found a significant positive relationship between nodule cover and megafaunal diversity in a more northern section of the UK1 claim area. This pattern is logical for epifauna because obligate hard substrate organisms will be absent in areas without nodules. However, why the presence of nodules would influence the diversity of highly mobile benthic scavengers/predators is unclear. The positive effects could be related to a greater abundance and diversity of potential epibenthic prey items since none of the taxa sampled are obligate scavengers. Nevertheless, this result suggests that nodule cover in the CCZ is important to the entire ecosystem, including the top predators. This finding should be considered when estimating the impact of future nodule mining activities on the CCZ community because obligate nodule fauna, infauna, epifauna, and the top predators and scavengers may all be negatively affected by the removal of nodules in the region.

The consistent significant and positive relationship of BPI with diversity, community composition, and the relative abundances of the top predators and scavengers, suggests that abyssal hills are important features in the CCZ ecosystem. The rarified number of species is higher for the abyssal hill stratum UK1 than for the featureless OMS stratum although these two strata are otherwise similar (overlying surface productivity and bottom temperature) and geographically proximate. In addition, fine-scale BPI was positively related to diversity. This supports the idea that there is higher species richness around abyssal hill features and implies that highly correlated topographic variables such as rugosity may also be important. Enhanced diversity and biomass is a paradigm of seamount ecology and seems to be well supported in the literature (Pitcher et al., 2007; Rowden et al., 2010). However, ecological studies on small, deep features like abyssal hills are still rare. Durden et al. (2015) examined the ecological impact of these features on megabenthos and reported significantly higher biomass and significantly different community composition, with higher densities of suspension feeders and surface deposit feeders on hill sites. Such patterns seem to hold true for scavengers in the CCZ as well. Our mixed model results suggest that BPI significantly affected relative scavenger abundances over the BPI gradient. *Plesiodiadema* sp., a deposit feeder and opportunistic scavenger had the strongest response to BPI. Interestingly, in both the Durden et al. (2015) dataset and the one presented here, *Munidopsis* sp. was exclusively found on abyssal hills.

The only other study to date examining the influence of abyssal hills on fish communities reported no difference in fish densities or distribution on the flank of a hill compared to the surrounding abyssal plain (Milligan et al., 2016). However, it is worth noting that this study had no AUV data from the top of the feature. Nevertheless, these findings contrast with those presented here and might suggest that topographic effects are of special significance to bait-attending fauna and not to all abyssal fishes. Interestingly, Milligan et al. did report over twice as many *Coryphaenoides armatus* individuals over the flank of the abyssal hill than the plain. There were also methodological differences because Milligan et al. (2016) tested for topographic effects on fish densities in a categorical fashion (“elevated terrain” versus “abyssal

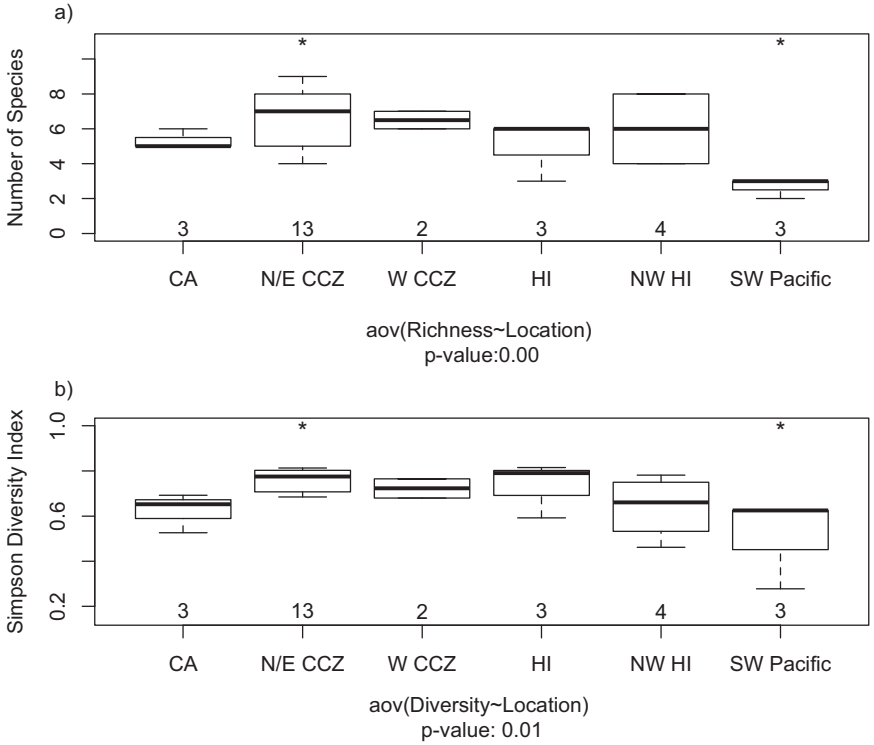

Fig. 7. a) A comparison of species richness among the different regions in this study along with data from the Californian slope (CAL, Yeh and Drazen, 2011), the Hawaiian Islands (Oahu) and the Northwestern Hawaiian Islands (Laysan Island, Pearl and Hermes Atoll; Yeh and Drazen, 2009), and from the Southwestern Pacific (Kermadec Trench; Jamieson et al., 2011). Sample size for each location is shown above x-axis. "*", "**', "***' indicate significantly different pairs as determined by and ANOVA with a Tukey HSD post hoc test. ANOVA significance is given in the subtitle. b) Simpson diversity compared amongst the different regions of those studies mentioned above.

plain"). This type of categorical examination of our own data also found no significant patterns. The authors also tested for differences in fish presence/absence based on distance to various depth contours (Milligan et al., 2016). Here we used BPI as a continuous topographic metric instead. Using BPI, which integrates bathymetric data over a larger spatial scale, we did detect an influence of abyssal hills on the bait-attending community. This illustrates that there is a continuum of change in diversity and community composition along topographic gradients, and that, as suggested by Milligan et al. (2016), the large spatial scales are likely the most important to these highly mobile predators.

These findings should be considered in the official creation of future marine reserve areas and provide supporting evidence for the inclusion of abyssal hills as an important habitat type for conservation as proposed in the current APEI system (Wedding et al., 2013). Though our results have shown some evidence that topography may be an important factor in structuring abyssal bait-attending communities, more feature-targeted sampling is required to identify direct biological drivers. Abyssal hills and seamounts taken together are the most abundant geological feature in the largest habitat on our planet, and we need to continue to build our understanding of the role and influence of these features on deep-sea benthic ecology.

4.3. Biogeography

This study is the first to describe the abyssal bait-attending community across the CCZ, and here we attempt to relate this community to the broader Pacific region. Jamieson et al. (2011)

Table 4
Abundance estimates for *Coryphaenoides* spp. for each deployment. T_{arr} abundance is the density as estimated from the time of first arrival model published by Priede et al. (1990). Note MaxN here is by deployment (drop-wise MaxN).

Drop	Stratum	Region	Swimming Speed (m/s)	T_{arr} (min)	T_{arr} Abundance Priede (fish/km^2)	MaxN (#)
CA01	UK1	Eastern CCZ	0.085	12	380	6
CA02	UK1	Eastern CCZ	0.082	89	10	5
CA03	OMS	Eastern CCZ	0.046	32	150	8
CA04	OMS	Eastern CCZ	0.064	20	440	3
CA05	OMS	Eastern CCZ	0.072	10	1530	8
CA06	UK1	Eastern CCZ	0.056	50	40	7
CA07	UK1	Eastern CCZ	0.072	42	100	8
CA08	UK1	Eastern CCZ	0.051	22	300	5
CA09	UK1	Eastern CCZ	0.094	10	1360	7
CA10	OMS	Eastern CCZ	0.088	42	90	2
CA11	OMS	Eastern CCZ	0.056	3	19,380	7
CA12	OMS	Eastern CCZ	0.130	30	90	2
CA13	APEI4	Northern CCZ	0.072	38	140	5
EQPAC_CA01	EQPAC1	Western CCZ	0.072	50	30	5
EQPAC_CA02	EQPAC2	Western CCZ	0.072	2	47,830	5

reported a low abundance, low diversity bait-attending assemblage from abyssal depths around the Kermadec Trench in the South West Pacific dominated by macrourids, as well as eels (Synaphobranchidae) and shrimps. Work done at Station M off the California coast has revealed a bait-attending community dominated by *C. armatus* with rare appearances of the ophidiid *Spectrunculus grandis*, and a study conducted on the eutrophic Californian slope at slightly shallower depths (3000 m) found a bait-attending community dominated by macrourids and zoarcids, along with the morid *Antimora* sp., one ophidiid species (*Spectrunculus* sp.), and crabs (*Paralomis* sp.) (Smith et al., 1997; Bailey et al., 2006; Yeh and Drazen, 2011). In contrast, on the Hawaiian slope and abyss (~3000–4700 m) bait-attending communities are dominated by ophidiids, eels (Synaphobranchidae), and aristeid shrimp, with only rare observations of *Coryphaenoides* spp. and zoarcids Yeh and Drazen, 2009). Therefore, the CCZ seems to host a community intermediate between the Californian macrourid/zoarcid community and the Hawaiian ophidiid/eel community, where taxa from each seem to be overlapping along with some unique, rare species such as Ophidiidae sp. 1, *Bathyonus caudalis*, *Pachcara nazca.*, a *Munidopsis* sp., and *Hymenopenaeus nereus*. In fact, the small decapod *H. nereus*, one of the most abundant scavengers in the CCZ, has not been seen since it was collected in the same area during the Albatross expedition in 1891 (pers. comm. M. Wicksten; Agassiz, 1892). In general, MaxNs of even dominant taxa are relatively low in the CCZ compared to Hawaii and California but similar to the southwest Pacific abyss (mean MaxN CCZ = 3.7; Hawaii = 5.3; California = 7.3; Kermadec = 2.3). Nevertheless, the CCZ community is relatively species rich and has a relatively high diversity, although the only significant difference is with the Kermadec area in the southwest Pacific (Fig. 7; Yeh and Drazen, 2009, 2011; Jamieson et al., 2011). A recent ROV study in a different stratum within the UK1 claim area also found high megafaunal abundance and richness compared to other abyssal habitats, including the California margin (Amon et al., 2016).

Our results also demonstrate the critical importance of further sampling in the APEI regions. Though the deployment in the "Area of Particular Environmental Interest" in the northern CCZ was only sampled once, the APEI had the lowest sampled species richness among the deployments (4, along with CA02 and CA03) and the lowest estimated number of species of any stratum in our dataset (Fig. 4a). The only other study to date that has sampled an APEI also reported lower densities for both mobile and sessile epifauna in the APEI (APEI 3) than in proximate claim areas (Vanreusel et al., 2016). Their results and our preliminary results highlight the need for more sampling, especially targeting APEIs, to evaluate their representivity for effective future environmental management of the CCZ.

Within the CCZ, the bait-attending community was different in the west than in either the east or north (Fig. 3). This difference was primarily driven by higher numbers of bait-attending ophidiids (especially *Bassozetus* and *Barathrites*) and lower dominance of the macrourid *Coryphaenoides* in the West. The difference seen for *Coryphaenoides* spp. could represent species distribution differences because *Coryphaenoides* spp. is more likely to be *C. yaquinae*, than *C. armatus* further away from the continental shelf. The overall regional differences reported here could also plausibly be the result of insufficient sampling in the West and the North. Nevertheless, the pattern found is consistent across various metrics (arrival curves, MaxN, total number observed). The decreased dominance of macrourids from east to west contradicts the prevalent idea that macrourids generally dominate the global abyssal bait-attending fauna (Priede et al., 1990; Armstrong et al., 1992; Thurston et al., 1995; Henriques et al., 2002; Yeh and Drazen, 2011).

Instead, this study, and other baited camera deployments, suggest that the picture is more complex, with dominance varying geographically between macrourids and ophidiids. For example, Armstrong et al. (1992) found clear differences in the bait-attending community at their more diverse oligotrophic station (MAP) versus their macrourid/eel dominated eutrophic stations (PAP) and attributed this to the presence of ophidiids at the oligotrophic station. They suggested that food availability may be the driving factor determining dominance and diversity in the North Atlantic abyss (Armstrong et al., 1992). Similarly, in the oligotrophic Hawaiian abyss macrourids were rare, and ophidiids dominated Yeh and Drazen, 2009). Fleury and Drazen (2013) reported an ophidiid-dominated community in the oligotrophic Sargasso Sea. These studies suggest that macrourids dominate in eutrophic areas but are replaced (perhaps outcompeted) by ophidiids in lower-productivity regimes further away from continental slopes. In a new abyssal-hadal depth zonation meta-analysis of baited camera deployments in the western Pacific, Linley et al. (2017) found that depth and the interplay of surface production and temperature together explained 36% of the variability in bait-attending communities across the region. They proposed that low surface productivity combined with higher bottom temperatures may be prohibitive energetically to *Coryphaenoides* spp.; in contrast, *Coryphaenoides* spp. may persist if high temperature is combined with high productivity, or low productivity is combined with low temperatures, enabling active foraging strategies characteristic of this group.

Though our modeling work did find a significant statistical effect of temperature, average surface chlorophyll was not significant. It is important to note that our data does not adequately sample the range of chlorophyll values across the CCZ, with most of the samples (12 of 15) being from two strata with similar production values (stratum averages = 0.143 vs 0.146 g/m^3). However, none of the three timescales of chlorophyll included in this study were significant. Our more oligotrophic western CCZ region was characterized by higher numbers and a persistent presence of ophidiids, rather than macrourids, attending bait; however, within the western areas there are two different productivity regimes. The less productive, warmer northwestern deployment (0.11 g chl/m^3; 1.50 °C) actually had fewer ophidiids and more macrourids than the more productive southwestern deployment (0.15 g chl/m^3; 1.44 °C), contrary to the prediction of Linley et al. (2017) (Table 1). This contradiction could be due to the small temperature and chlorophyll ranges in our dataset, or perhaps this hints at the importance of other factors beyond temperature and chlorophyll such as topography or a direct measure of food availability at depth. For example, Janßen et al. (2000) reported that macrourids were rare in the bait-attending community of the Arabian Sea, independent of local productivity, with the community instead consistently dominated by ophidiids, amphipods, zoarcids, and aristeid shrimps.

Our models did identify the statistically significant effects of temperature, topographic predictors (BPI), and current characteristics. Current speed was a significant factor in determining scavenger MaxN, in contrast to the findings by Linley et al. (2017) who reported no significant effect of current speeds on community structure across depth gradients. Strong effects of depth on community composition across abyssal-hadal boundaries may overshadow the effects of current characteristics whose effects may only be significant within a single depth zone. The emerging large-scale geographic differences in abyssal bait-attending communities may be driven by topography, current characteristics, and depth, in addition to temperature and surface-productivity gradients.

An alternative explanation for the spatial patterning we observed within the CCZ could be seasonality effects. Interannual variation in nutritional condition and population dynamics of macrourids have been reported, and some authors even suggest seasonal basin-scale migration behavior (Smith et al., 1997, Drazen 2002, Bailey et al., 2006, Drazen and Haedrich, 2012). Seasonal effects cannot be ruled out here because the western deployments were conducted in the late summer, and the eastern and northern deployments were conducted in the spring. A long term baited camera time series would be required to test this hypothesis.

5. Conclusion

We have described the megafaunal bait-attending community of the CCZ for the first time in detail using baited camera techniques, and examined topographic and environmental influences on this community. Macrourids tend to dominate at bait, and variations in their size are related to a combination of topographic (BPI), environmental (temperature and nodule cover), and oceanographic (current direction) factors. Overall, it seems that the CCZ bait-attending community may be a relatively diverse, low abundance assemblage, intermediate in taxonomic structure between the Hawaiian ophidiid-dominated and the Californian macrourid- and zoarcid-dominated abyssal bait-attending communities. Moreover, community differences exist within the CCZ itself, and these differences should be considered in future environmental management plans for the region. More sampling is needed, especially in APEI areas, to rigorously examine these ideas. We have found a continuum of change in the abundances of bait-attending taxa along BPI gradients suggesting that abyssal hills have a positive influence on scavenger diversity and community composition in the CCZ. Finally, nodule cover also had a positive influence on the length of the dominant scavenger/predator as well as the diversity of the bait-attending fauna. Finally, we have identified a link between nodule cover and scavengers. Though the mechanisms and drivers behind this link are unclear, this suggests that mining activities will impact all levels of the CCZ ecosystem including the scavengers and top predators.

Funding

This work was supported by UK Seabed Resources, LTD contract no. SRD100100. UK Seabed Resources had no role in the study design, data collection and analysis, decision to publish, or preparation of the manuscript.

Acknowledgements

The authors would like to acknowledge the Sexton Co. for the custom design of the DeepCam system. Many thanks to the captain and crew of the R/V Thompson and the captain and crew of the R/V Kilo Moana. Thank you to Dr. Chris Kelley and Virginia Moriwake for help with the bathymetric grid analyses. Thank you to Dr. Margaret McManus for help with ACDP data processing and analysis. Thank you to Dr. Clifton C. Nunnally, Dr. Andrew Sweetman, Oliver Kersten, Kirstin Meyer and all the Abyssline team members for assistance at sea. Thank you also to Dr. Eric Anderson for the morphological identification of the *Pachycara nazca* specimens. This is SOEST contribution number 10008.

Appendix A. Supporting information

Supplementary data associated with this article can be found in the online version at http://dx.doi.org/10.1016/j.dsr.2017.04.017.

References

Agassiz, A., 1892. General Sketch of the Expedition of the “Alabtross” from February to May. Museum Comp. Zool. Harvard Collpp. 1891.
Amon, D.J., Ziegler, A.F., Dahlgren, T.G., Glover, A.G., Goineau, A., Gooday, A.J., Wiklund, H., Smith, C.R., 2016. Insights into the abundance and diversity of abyssal megafauna in a polymetallic-nodule region in the eastern Clarion-Clipperton Zone. Sci. Rep. **6**, 30492.
Armstrong, J.D., Bagley, P.M., Priede, I.G., 1992. Photographic and acoustic tracking observations of the behaviour of the grenadier Coryphaenoides (Nematonurus) armatus the eel Synaphobranchus bathybius, and other abyssal demersal fish in the North Atlantic Ocean. Mar. Biol. **112**, 535–544.
Bailey, D.M.D., King, N.N.J., Priede, I.G.I., 2007a. Cameras and carcasses: historical and current methods for using artificial food falls to study deep-water animals. Mar. Ecol. Prog. Ser. **350**, 179–191.
Bailey, D.M., Ruhl, H.A., Smith, K.L., 2006. Long-term change in benthopelagic fish abundance in the abyssal northeast Pacific Ocean. Ecology **87**, 549–555.
Bailey, D.M., Wagner, H.J., Jamieson, A.J., Ross, M.F., Priede, I.G., 2007b. A taste of the deep-sea: The roles of gustatory and tactile searching behaviour in the grenadier fish Coryphaenoides armatus. Deep. Res. Part I Oceanogr. Res. Pap **54**, 99–108.
Barton, K., 2016. MuMIn: Multi-Model Inference.
Bates, D., Maechler, M., Bolker, B., Walker, S., 2015. Fitting Linear Mixed-Effects Models Using {lme4}. J. Stat. Software2 **67**, 1–48.
Cappo, M., Harvey, E.S., Shortis, M., 2006. Counting and measuring fish with baited video techniques – an overview. Australian Society for Fish Biology Workshop Proceedings 101–114.
Carter, G.S., Gregg, M.C., Merrifield, M. a, 2006. Flow and Mixing around a Small Seamount on Kaena Ridge, Hawaii. J. Phys. Oceanogr. **36**, 1036–1052.
Clark, M.R., 2009. Deep-sea seamount fisheries: a review of global status and future prospects. Lat. Am. J. Aquat. Res **37**, **3**.
Cribari-Neto, F., Zeileis, A., 2010. Beta Regression in R. J. Stat. Softw **34**, 1–24.
Danovaro, R., Aguzzi, J., Fanelli, E., Billett, D., Gjerde, K., Jamieson, A., Ramirez-Llodra, E., Smith, C.R., Snelgrove, P.V.R., Thomsen, L., Van Dover, C.L., 2017. An ecosystem-based deep-ocean strategy. Science (80-.) **355**, 452–454.
Drazen, J.C., 2002. Energy budgets and feeding rates of Coryphaenoides acrolepis and C. armatus. Mar. Biol. **140**, 677–686.
Drazen, J.C., Haedrich, R.L., 2012. A continuum of life histories in deep-sea demersal fishes. Deep. Res. Part I Oceanogr. Res. Pap **61**, 34–42.
Drazen, J.C., Popp, B.N., Choy, C.A., Clemente, T., De Forest, L., Smith Jr, K.L., Smith, K.L.J., 2008. Bypassing the abyssal benthic food web: Macrourid diet in the eastern North Pacific inferred from stomach content and stable isotopes analyses. Limnol. Oceanogr. **53**, 2644.
Durden, J.M., Bett, B.J., Jones, D.O.B., Huvenne, Va.I., Ruhl, Ha, 2015. Abyssal hills – hidden source of increased habitat heterogeneity, benthic megafaunal biomass and diversity in the deep sea. Prog. Oceanogr. **137**, 209–218.
Genin, A., 2004. Bio-physical coupling in the formation of zooplankton and fish aggregations over abrupt topographies. J. Mar. Syst. **50**, 3–20.
Genin, A., Dayton, P.K., Lonsdale, P.F., Spiess, F.N., 1986. Corals on seamount peaks provide evidence of current acceleration over deep-sea topography. Nature **322**, 59.
Genin, A., Dower, J.F., 2007. Seamount plankton dynamics. *In* Seamounts: ecology, fisheries and conservation 85–100.
Gotelli, N.J., Colwell, R.K., 2001. Quantifyinf Biodiversity: Procedures and Pitfalls in the Measurement and Comparison of Species Richness. Ecol. Lett **4**, 379–391.
Harris, P.T., Macmillan-Lawler, M., Rupp, J., Baker, E.K., 2014. Geomorphology of the oceans. Mar. Geol. **352**, 4–24.
Henriques, C., Priede, I.G., Bagley, P.M., 2002. Baited camera observations of deep-sea demersal fishes of the northeast Atlantic Ocean at 15-28??N off West Africa. Mar. Biol. **141**, 307–314.
Hubbs, C.L., 1959. Initial discoveries of fish faunas on seamounts and offshore banks in the eastern Pacific. Pac. Sci. **12**, 311.
Jackson, M.M., Turner, M.G., Pearson, S.M., Ives, A.R., 2012. Seeing the forest and the trees: multilevel models reveal both species and community patterns. Ecosphere **3**, Article 79.
Jamieson, A.J., Priede, I.G., Craig, J., 2012. Distinguishing between the abyssal macrourids Coryphaenoides yaquinae and C. armatus from in situ photography. Deep Sea Res. Part I Oceanogr. Res. Pap **64**, 78–85.
Jamieson, a J., Kilgallen, N.M., Rowden, a a, Fujii, T., Horton, T., Lörz, a N., Kitazawa, K., Priede., I.G., 2011. Bait-attending fauna of the Kermadec Trench, SW Pacific Ocean: Evidence for an ecotone across the abyssal-hadal transition zone. Deep. Res. Part I Oceanogr. Res. Pap **58**, 49–62.
Janßen, F., Treude, T., Witte, U., 2000. Scavenger assemblages under diff ering trophic conditions: a case study in the deep Arabian Sea. Deep Sea Res. Part II Top. Stud. Oceanogr **47**, 2999–3026.
Kim, S.-S., Wessel, P., 2011. New global seamount census from altimetry-derived gravity data. Geophys. J. Int **186**, 615–631.
Lavelle, J.W., Mohn, C., 2010. Motion, Commotion, and Biophysical Connections at Deep Ocean Seamounts. Oceanography **23**, 90–103.
Linley, T.D., Stewart, A.L., McMillan, P.J., Clark, M.R., Gerringer, M.E., Drazen, J.C., Fujii, T., Jamieson, A.J., 2017. Bait attending fishes of the abyssal zone and hadal boundary: community structure, functional groups and species distribution in the Kermadec. New Hebrides and Mariana trenches. Deep Sea Res. Part I Ocean. Res. Pap. **121**.
Lutz, M.J., Caldeira, K., Dunbar, R.B., Behrenfeld, M.J., 2007. Seasonal rhythms of net primary production and particulate organic carbon flux to depth describe the efficiency of biological pump in the global ocean. J. Geophys. Res. **112**, C10011.
McClain, C.R., 2007. Seamounts: Identity crisis or split personality? J. Biogeogr.
Mewes, K., Mogollón, J.M., Picard, A., Rühlemann, C., Kuhn, T., Nöthen, K., Kasten, S., 2014. Impact of depositional and biogeochemical processes on small scale variations in nodule abundance in the Clarion-Clipperton Fracture Zone. Deep Sea Res. Part I Oceanogr. Res. Pap **91**, 125–141.
Milligan, R.J., Morris, K.J., Bett, B.J., Durden, J.M., Jones, D.O.B., Robert, K., Ruhl, H.A., Bailey, D.M., 2016. High resolution study of the spatial distributions of abyssal fishes by autonomous underwater vehicle. Sci. Rep. **6**, 1–12.
Oksanen, J., F. G. Blanchet, R. Kindt, P. Legendre, P. R. Minchin, R. B. O’Hara, G. L. Simpson, P. Solymos, M. H. H. Stevens, and H. Wagner. 2015. vegan: Community Ecology Package.
Pearcy, W.G., Ambler, J.W., 1974. Food habits of deep-sea macrourid fishes off the Oregon coast. Deep Sea Res. Oceanogr. Abstr **21**, 745–759.
Pitcher, T.J., Morato, T., Hart, P.J.B., Clark, M.R., Haggan, N., Santos, R.S., 2007. Seamounts: ecology, fisheries & conservation. Wiley. com, Oxford, UK.
Priede, I.G., Godbold, J. a, King, N.J., Collins, M. a, Bailey, D.M., Gordon, J.D.M., 2010. Deep-sea demersal fish species richness in the Porcupine Seabight. Mar. Ecol. **31**. Global and regional patterns, NE Atlantic Ocean, pp. 247–260.

Priede, I.G., Merrett, N.R., 1996. Estimation of abundance of abyssal demersal fishes; a comparison of data from trawls and baited cameras. J. Fish Biol. **49**, 207–216.
Priede, I.G., Smith, K.L., Armstrong, J.D., 1990. Foraging behavior of abyssal grenadier fish: inferences from acoustic tagging and tracking in the North Pacific Ocean. Deep Sea Res. Part A. Oceanogr. Res. Pap **37**, 81–101.
Rowden, A.A., Dower, J.F., Schlacher, T.A., Consalvey, M., Clark, M.R., 2010. Paradigms in seamount ecology: fact, fiction and future. Mar. Ecol **31**, 226–241.
Saefken, B., D. Ruegamer, S. Greven, and T. Kneib. 2014. cAIC4: Conditional Akaike information criterion for lme4.
Sainte-Marie, B., Hargrave, B.T., 1987. Estimation of Scavenger Abundance and Distance of Attraction to Bait. Mar. Biol. **94**, 431–443.
Sappington, J.M., Longshore, K.M., Thompson, D.B., 2007. Quantifying Landscape Ruggedness for Animal Habitat Analysis: A Case Study Using Bighorn Sheep in the Mojave Desert. J. Wildl. Manage. **71**, 1419–1426.
Smith, A., Priede, I.G., Bagley, P.M., Addison, S.W., 1997. Interception and dispersal of artificial food falls by scavenging fishes in the abyssal Northeast Atlantic: Early-season observations prior to annual deposition of phytodetritus. Mar. Biol. **128**, 329–336.
Smith, C.R., Demopoulos, A.W., 2003. The deep Pacific ocean floor. *In* Ecosystems of the Deep Oceans Volume 28, 179–218.
Smith, C.R., De Leo, F.C., Bernardino, A.F., Sweetman, A.K., Arbizu, P.M., 2008. Abyssal food limitation, ecosystem structure and climate change. Trends Ecol. Evol. **23**, 518–528.
Thurston, M.H., Bett, B.J., Rice, A.L., 1995. Abyssal Megafaunal Necrophages: Latitudinal Differences in the Eastern North Atlantic Ocean. Int. Rev. der gesamten Hydrobiol. und Hydrogr **80**, 267–286.
Trenkel, V.M., Lorance, P., Mahévas, S., 2004. Do visual transects provide true population density estimates for deepwater fish. ICES J. Mar. Sci. J. du Cons **61**, 1050–1056.
Turnewitsch, R., Lahajnar, N., Haeckel, M., Christiansen, B., 2015. An abyssal hill fractionates organic and inorganic matter in deep-sea surface sediments. Geophys. Res. Lett. **42**, 7663–7672.
Vanreusel, A., Hilario, A., Ribeiro, P.A., Menot, L., Arbizu, P.M., 2016. Threatened by mining, polymetallic nodules are required to preserve abyssal epifauna. Sci. Rep. **6**, 26808.
Wedding, L.M., Friedlander, A.M., Kittinger, J.N., Watling, L., Gaines, S.D., Bennett, M., Hardy, S.M., Smith, C.R., 2013. From principles to practice: a spatial approach to systematic conservation planning in the deep sea. Proc. Biol. Sci. **280**, 20131684.
Wedding, L.M., Reiter, S.M., Smith, C.R., Gjerde, K.M., Kittinger, J.N., Friedlander, a M., Gaines, S.D., Clark, M.R., Thurnherr, a M., Hardy, S.M., Crowder, L.B., 2015. Managing mining of the deep seabed. Science (80-.) **349**, 144–145.
Wessel, P., 2007. Seamount characteristics. *In* Seamounts: Ecology, Fisheries & Conservation 3–25.
Wright, D. J., M. Pendleton, J. Boulware, S. Walbridge, B. Gerlt, D. Eslinger, D. Sampson, and E. Huntley. 2012. ArcGISBenthic Terrain Modeler (BTM), v. 3.0.
Wyrtki, K., 1961. The Thermohaline Circulation in Relation to the General Circulation in the Oceans. Deep. Res. Part I **8**, 39–64.
Yeh, J., Drazen, J.C., 2009. Depth zonation and bathymetric trends of deep-sea megafaunal scavengers of the Hawaiian Islands. Deep. Res. Part I Oceanogr. Res. Pap **56**, 251–266.
Yeh, J., Drazen, J.C., 2011. Baited-camera observations of deep-sea megafaunal scavenger ecology on the California slope. Mar Ecol Prog Ser **424**, 145–156.
Yesson, C., Clark, M.R., Taylor, M.L., Rogers, A.D., 2011. Deep-Sea Research I The global distribution of seamounts based on 30 arc seconds bathymetry data. Deep. Res. Part I **58**, 442–453.
Zuur, A.F., Ieno, E.N., Elphick, C.S., 2010. A protocol for data exploration to avoid common statistical problems. Methods Ecol. Evol **1**, 3–14.